General and Inorganic Chemistry

Modeling heat and mass transfer in the gas-phase chemical deposition of polycrystalline ZnSe layers

V. G. Minkina

A. V. Lykov Heat and Mass Transfer Institute, Academy of Science of Belorussia, 15 ul. P. Brovki, 220072 Minsk, Belarus'
Fax: 007 (017 2) 32 2513. E-mail: allusr@avtlab.itmo.minsk.by

Heat and mass transfer in the gas-phase deposition of zinc selenide in the zinc—hydrogen selenide—argon system with separate injection of reagents into a reactor by local jets has been studied. The effects of technological parameters, design, and the geometric dimensions of the reactor on the distribution of the deposition rates of the zinc selenide layers formed have been considered.

Key words: heat and mass transfer, zinc selenide, hydrogen selenide, deposition rate.

Improvements in optical techniques are determined in many respects by the development of the technology of the growth of zinc selenide layers. To upgrade the quality of deposited zinc selenide layers, it is necessary to prevent the interaction of the initial reagents outside the reaction zone and to vary the rate at which they are fed. The mathematical models of the gas-phase deposition of zinc selenide are few and contain many assumptions and simplifications. For example, for modeling mass transfer in a reactor[1] it has been assumed[2,3] that all gases were mixed before injection into the reactor and that they were injected at a uniform concentration and temperature over the whole cross section; the nonuniformity of the temperature field in the reactor was not taken into account, and the rate profile along the reactor was considered unchanged[2] or completely developed.[3] In Ref. 4, data on the substantial role of chemical kinetic factors during the interaction of Zn vapor with H_2Se in a H_2 flow were obtained; however, the reaction rate constant was not determined. Both kinetic and diffusion or intermediate reaction regimes were observed for the deposition of polycrystalline ZnSe layers in an Ar flow. At low temperatures (≤873 K) the reaction order is 0.5 with respect to H_2Se. This contradicts the data of Ref. 5, according to which the order with respect to H_2Se is equal to 1. The first data on the rate constant of the overall heterogeneous reaction in a wide temperature range, from 774 to 1146 K, were published in Refs. 3, 5, and 6. These data were obtained using a very simplified mathematical model of mass transfer, which assumed a uniform concentration of H_2Se in the inlet cross section of the reactor, a constant flow rate along the reactor, and the absence of convective lateral mass transfer and a temperature gradient. These are not the conditions that exist in a real reactor.

Mathematical model of heat and mass transfer

1. Equations of conservation

A numerical analysis of the gas-phase deposition of zinc selenide from a $Zn—H_2Se—Ar$ mixture with separate injection of the reagents by local jets is performed in this work. The scheme of the reactor is presented in Fig. 1. The ratio of the height of the reactor to its width is considerably greater than unity, which makes it pos-

Translated from *Izvestiya Akademii Nauk. Seriya Khimicheskaya*, No. 7, pp. 1625—1631, July, 1996.

1066-5285/96/4507-1535 $15.00

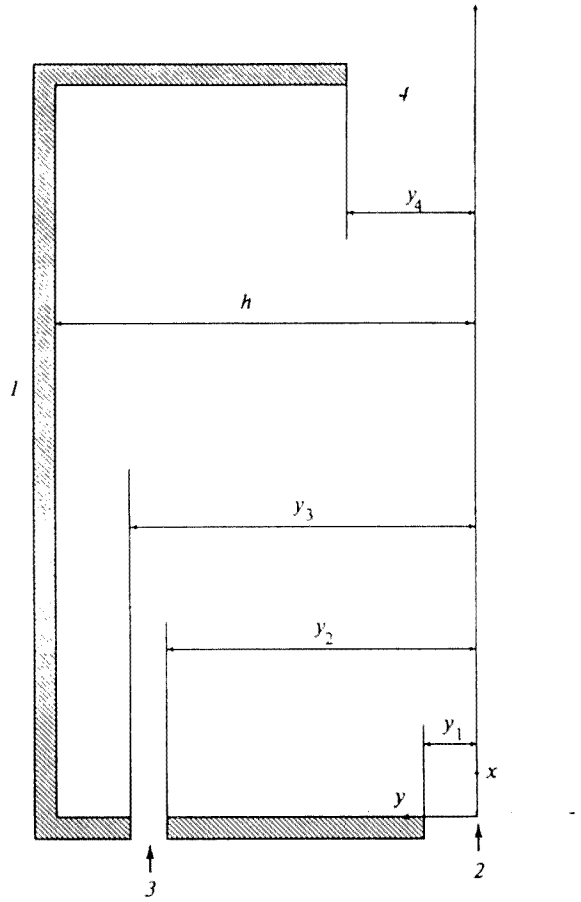

Fig. 1. Scheme of the vertical flow-type reactor: *1*, walls of the reactor; *2* and *3*, inlet ports; and *4*, outlet ports.

sible to consider the flow and heat and mass transfer in the reactor to be two-dimensional rather than three-dimensional. The development of the profiles of the rate, temperature, and concentrations of the components of the vapor-gas mixture (VGM) in the reactor is taken into consideration. Hydrogen selenide is injected into the central slit, and the zinc vapor is conveyed peripherally. Argon is used as the carrier-gas. A ZnSe layer is deposited on the heated walls of the reactor according to the stoichiometric equations

$$Zn_{(g)} + H_2Se = ZnSe_{(s)} + H_2, \quad (1)$$

$$2\ ZnSe_{(s)} = 2\ Zn_{(g)} + Se_2. \quad (2)$$

The process of the gas-phase deposition of ZnSe is described by a system of Navier—Stokes type equations of the conservation of momentum, energy, and mass:

$$\frac{\partial}{\partial x}\left(\omega\frac{\partial\Psi}{\partial y}\right) - \frac{\partial}{\partial y}\left(\omega\frac{\partial\Psi}{\partial x}\right) - \frac{\partial^2}{\partial x^2}(\mu\omega) - \frac{\partial^2}{\partial y^2}(\mu\omega) + g\frac{\partial\rho}{\partial y} = 0, \quad (3)$$

$$\frac{\partial}{\partial x}\left(\frac{1}{\rho}\frac{\partial\Psi}{\partial x}\right) + \frac{\partial}{\partial y}\left(\frac{1}{\rho}\frac{\partial\Psi}{\partial y}\right) + \omega = 0, \quad (4)$$

$$\frac{\partial}{\partial x}\left(H\frac{\partial\Psi}{\partial y}\right) - \frac{\partial}{\partial y}\left(H\frac{\partial\Psi}{\partial x}\right) - \frac{\partial}{\partial x}\left(\frac{\lambda_T}{C_p}\frac{\partial H}{\partial x}\right) - \frac{\partial}{\partial y}\left(\frac{\lambda_T}{C_p}\frac{\partial H}{\partial y}\right) = 0, \quad (5)$$

$$\frac{\partial}{\partial x}\left(C_i\frac{\partial\Psi}{\partial y}\right) - \frac{\partial}{\partial y}\left(C_i\frac{\partial\Psi}{\partial x}\right) - \frac{\partial}{\partial x}\left(\rho D_i\frac{\partial C_i}{\partial x}\right) - \frac{\partial}{\partial y}\left(\rho D_i\frac{\partial C_i}{\partial y}\right) = 0, \quad (6)$$

where x and y are the longitudinal and lateral coordinates, respectively; ω is the vortex strength; Ψ is the current function; μ is the viscosity coefficient; g is acceleration of free fall; ρ is density; H is enthalpy; λ_T is the heat conductivity coefficient; C_p is the heat capacity coefficient; C_i is the weight concentration of the ith component; and D_i is the diffusion coefficient of the ith component.

The system of differential equations was solved by the method of finite differences according to the described procedure.[7] The dependences of the physical properties of the gas mixture (diffusion coefficients, heat capacity, heat conductivity, viscosity, and density) on the temperature, pressures, and chemical composition were taken into account.[8—10]

The dynamic viscosity coefficient for the gas was calculated by the Sutherland formula:[8]

$$\mu_i = \mu_{0i}\frac{273 + S_i}{T + S_i}(T/273)^{1.5},$$

where S_i is the Sutherland constant of the ith component and μ_{0i} is the dynamic viscosity coefficient of the ith component at 0 °C.

The viscosity of the gas mixture (μ_{mix}) was determined by the Wilk formula[10]

$$\mu_{mix} = \sum_{i=1}^{6}\mu_i \Big/ \left(1 + \frac{1}{X_i}\sum\Phi_{ij}X_j\right),$$

where Φ_{ij} is the function of the viscosity and molecular weights of the individual components

$$\Phi_{ij} = [1 + (\mu_i/\mu_j)^{0.5}(M_j/M_i)^{0.25}]^2/[8(1 + M_i/M_j)^{0.5}],$$

where M_i and M_j are the molecular weights of the components, and X_i and X_j are the molar fractions of the components in the gas mixture.

By analogy with viscosity, the diffusion coefficients for the binary mixture were calculated by the Sutherland formula

$$D_{ij} = D_{ij}^0\frac{273 + S_{ij}}{T + S_{ij}}(T/273)^{2.5},$$

where D_{ij}^0 is the diffusion coefficient of the ith component in the jth component at 0 °C. The Wilk formula,

which gives exact results, was used for the calculation of the diffusion coefficients of the multicomponent system

$$D_i = (1 - X_i)/\Sigma X_j/D_{ij}.$$

Equations (3)—(6) are supplemented by boundary conditions.

2. Boundary conditions

Let us consider the boundary conditions that Eqs. (3)—(6) describing two-dimensional flows must satisfy.

The current function Ψ and vortex strength ω at the inlet of the reactor have the form:

in the central port (from the axis to y_1)

$$\Psi = \int_0^{y_1} \rho u dy, \quad \omega = \frac{\partial v}{\partial x} - \frac{\partial u}{\partial y}, \tag{7}$$

in the peripheral port (from y_2 to y_3)

$$\Psi = \int_{y_2}^{y_3} \rho u dy + \Psi(y_1), \quad \omega = \frac{\partial v}{\partial x} - \frac{\partial u}{\partial y} \tag{8}$$

(u and v are the longitudinal and lateral components of the flow rate of the gas mixture; for y_1, y_2, and y_3, see Fig. 1).

In the outlet port and on the symmetry plane of the reactor $\partial F/\partial y = 0$ and $\partial F/\partial x = 0$, respectively (here F are the desired variables). The current function on the wall from y_1 to y_2, $\Psi = \Psi(y_1)$; from y_3 to h, $\Psi = \rho_0 u_0 h$; and on the side and upper walls, $\Psi = \rho_0 u_0 h_0$ (for h, see Fig. 1). The boundary conditions for the vortex strength on the walls were determined from the condition that the change in ω along a line normal to the wall is linear[7]

$$\omega = -\left[\frac{3(\Psi_{np} - \Psi_p)}{h_{np}^2 \rho} - \frac{\omega_{np}}{2}\right], \tag{9}$$

where p is a point on the wall, np is the nearest node of the framework along a line normal to it, and h_{np} is the distance between them.

Since reliable data on chemical kinetics are scarce (see Refs. 11—13), it was assumed in this work that a thermodynamic quasi-equilibrium exists on the deposition surface. The concentrations of the components on the walls of the reactor were calculated from the condition of the thermodynamic quasi-equilibrium, taking into account the balance of mass flow. As shown by the thermodynamic analysis of the Zn—H_2Se—Ar—H_2 system using the data of Refs. 14 and 15 in the temperature range from 700 to 1500 K and at pressures from 1 to 100 kPa, the main components of the equilibrium gas mixture are H_2Se, Zn, H_2, Se_2, and Ar. The other components (HSe, ZnH, and Se_i, where i = 3—8) are present in negligible amounts. The equilibrium partial pressures of Zn and H_2Se are considerably lower than the partial pressures of these substances in the VGM at the inlet of the reactor. From the equations of reactions (1) and (2) we have for the equilibrium constants

$$K_1 = P_4/(P_1 P_2), \quad K_2 = P_1^2 P_5,$$

where indices 1, 2, 4, and 5 correspond to Zn, H_2Se, H_2, and Se_2, respectively.

Thermodynamic data from Ref. 16 were used to determine the values of K. Since the total pressure of the mixture P_0 is constant, $P_0 = \sum_{i=1}^{5} P_i$. The expression of equality of the flow of Zn and Se atoms on the deposition surface, *i.e.*, the condition of stoichiometry, has the form

$$\frac{D_1}{M_1}\frac{\partial C_1}{\partial y} = \frac{D_2}{M_2}\frac{\partial C_2}{\partial y} + 2\frac{D_5}{M_5}\frac{\partial C_5}{\partial y}$$

For the purposes of approximation, let us use the value of the rate constant of the heterogeneous reaction presented previously[6] k = 0.085 m s^{-1}, at the lateral reactor dimension h = 0.25 m, deposition temperature 1023 K, total pressure 2.66 kPa, and concentrations of Zn and H_2Se vapor in the VGM 0.1 molar fractions. Then we obtain for the value of the dimensionless complex $\lambda = 2kh/D$ = 12.5 (D is the diffusion coefficient of the limiting component in the VGM). This value of λ corresponds to an intermediate diffusion-kinetic regime of the limiting heterogeneous reaction.[17]

For the preparation of high-grade layers, it is desirable to work under conditions such that when reagents are transferred in the gas phase as individual molecules, not clusters, the formation of a powder in the reactor should be excluded. The critical temperature-dependent values of the concentration of H_2Se, exceeding which results in the formation of powder, are presented in Ref. 18. When the deposition temperature increases from 850 to 1050 K, the critical concentration of H_2Se decreases approximately from $10 \cdot 10^{-5}$ to $4 \cdot 10^{-5}$ mol L^{-1}. Since the nucleation is determined by the temperature, concentration, and flow rate fields, which depend on the design of the reactor, its dimensions, and consumptions of gases, the data presented[18] can be considered as tentative. The diffusion coefficients for the limiting component of the VGM at various temperatures were calculated[5] from the experimentally determined distribution of the deposited layer thickness along the reactor and the mathematical model of heat and mass transfer considered above. The diffusion coefficient increases and then decreases as the temperature increases from 700 to 950 K. This effect is explained by the change in the mechanism of deposition: below 950 K the reagents diffuse to the deposition surface as molecules, while above 950 K the deposition mainly occurs due to the formation of clusters $(-ZnSe-)_n$ in the reaction volume, whose diffusion coefficient is much lower than that of H_2Se. The simplified character of the

mathematical model may cause quantitative errors. Therefore, the question of the change in the deposition mechanism as the temperature increases should be additionally studied.

The transfer of reagents as individual molecules is considered in this work. At the same time, it was kept in mind that the deposition temperature, the concentrations of reagents, and the total pressure could not be higher than the experimentally confirmed values.

Results of numerical studies

1. Development of fields of flow rate, temperature, and concentration

Pronounced maxima in the rate are observed opposite the inlet nozzles at 1.33 kPa in the bottom part of the reactor. Traces from the ports become smooth, and the rate profile begins to gain the form typical of flow in a channel as the distance from the inlet increases. The effect of free convection on the flow of the VGM is manifested in the transformation of the central maximum of the rate to a minimum, because a portion of the gas is diverted from the center to the periphery, involving vertical motion along the reactor walls. This tendency increases as the pressure increases. At 5.32 kPa the rate maxima near the inlet ports decrease, and the flow rate gains a negative sign, *i.e.*, recirculation appears at some distance from the inlet in the region of the symmetry plane of the reactor (Fig. 2). Reverse flow appears in the central part of the reactor, while the direct flow is pressed against the walls. A further increase in the total pressure results in the development of a recirculation zone and the acceleration of the flow along the wall. The traces from the inlet ports disappear even at short distances from the ports, which attests to a weak effect of the arrangement of the ports at the inlet of the reactor during intense recirculation.

The average effect of pressure on the rate profile along the reactor is shown in Fig. 3. At 0.665 kPa the rate profile has a maximum on the symmetry axis, which is characteristic of flow in a channel in the absence of free convection or with a weak convection effect, while at 2.66 kPa there is a pronounced minimum on the symmetry axis and a maximum near the wall. Recirculation near the symmetry axis and an increase in the maximum of the rate near the wall are observed at 5.32 kPa.

The role of free convection depends on the pressure and other values, for example, on the consumption and temperature of the VGM, dimensions of the reactor, *etc.* A decrease in the consumption of the VGM affects the form of the rate profile in a way that is qualitatively similar to the effect of an increase in the pressure. Decreasing the temperature of the hydrogen selenide—argon mixture from 823 to 373 K sharply changes the rate profile resulting in recirculation (Fig. 4). Decreasing the cross section of the reactor suppresses free convection and acts as an increase in the consumption of the VGM or a decrease in the pressure.

Decreasing the size of the outlet port y_4 from $0.34h$ to $0.06h$ in the absence of recirculation changes the rate profile several percentage units to make it more flat, decreasing the flow rate in the region of the symmetry plane and increasing it near the walls of the reactor.

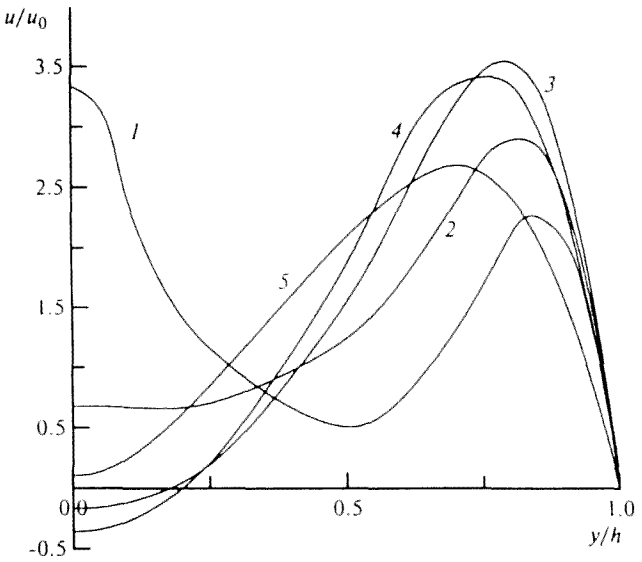

Fig. 2. Development of the profile of the flow rate of the VGM over the cross section of the reactor, x/cm: 6 (*1*), 30 (*2*), 60 (*3*), 90 (*4*), 106 (*5*); $T_1 = T_2 = 823$ K, $P_0 = 5.32$ kPa, $h = 25$ cm, $G = 2.5$ m^3 h. Index "0" corresponds to the inlet of the reactor, G is the consumption of the VGM.

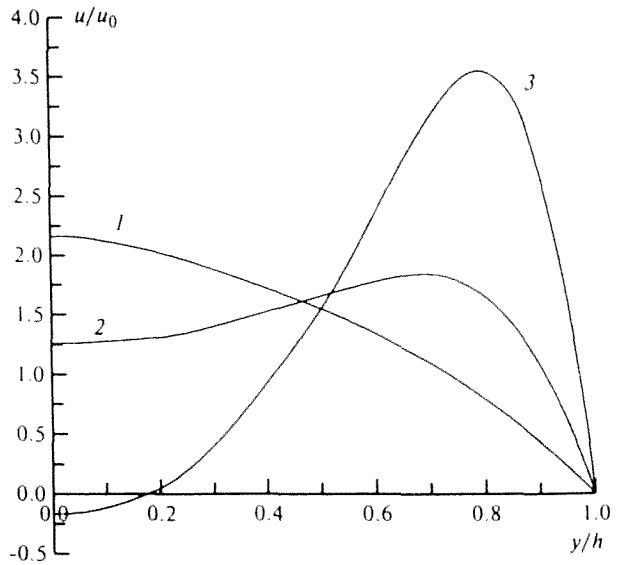

Fig. 3. Development of the profile of the flow rate of the VGM over the cross section of the reactor at various pressures, P_0/kPa: 0.665 (*1*), 2.66 (*2*), 5.32 (*3*). $x = 60$ cm (for designations, see Fig. 2).

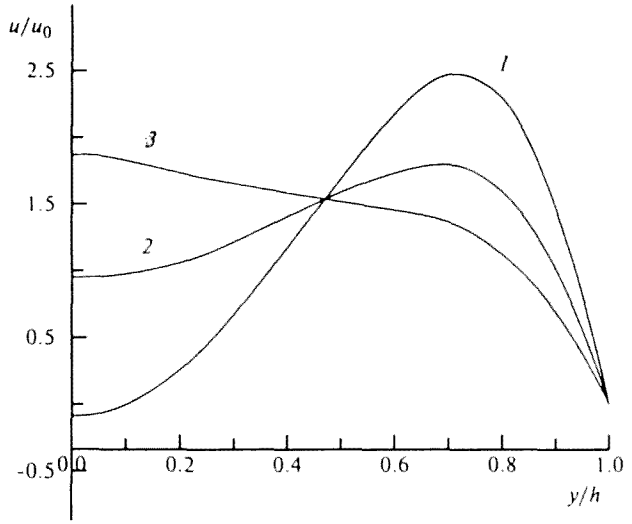

Fig. 4. Development of the profile of the flow rate of the VGM over the cross section of the reactor at various temperatures of H_2Se at the inlet, T_2/K: 373 (*1*), 573 (*2*), 823 (*3*). T_1 = 823 K, P_0 = 2.66 kPa, G = 5 m^3 h, x = 84 cm.

Constricting the inlet ports from $0.06h$ to $0.01h$ somewhat sharpens the rate maxima near the injection points, but this effect disappears as the distance from the inlet increases, because the Reynolds numbers are very small. The change in the rate caused by the constriction of the ports was not greater than several percentage units. It is evident that the relative removal of the peripheral jet y_{23}/h (y_{23} is the distance from the axis to the middle of the peripheral port) in the absence of recirculation strongly affects the rate profile in the bottom part of the reactor. When the peripheral jet of zinc flows along the wall of the reactor, it acts as a gas curtain intercepting hydrogen selenide from the deposition surface. As mentioned, intense recirculation abolishes this effect.

As it moves away from the inlet, the gas gradually warms up, its average temperature increases, and the temperature gradient on the wall of the reactor decreases. As the pressure increases and the consumption of the VGM decreases, the temperature distribution over the cross section of the reactor becomes more uniform because of stirring of the gas due to the recirculation (Fig. 5).

The concentrations of zinc and hydrogen selenide decrease as the VGM moves to the outlet. A large excess of zinc over H_2Se is observed on the deposition surface. This excess can be explained by the fact that the reagents were not stirred beforehand, but were injected separately into the reactor, and the zinc jet was located closer to the deposition surface. Changes in the pressure in the reactor and in the consumption of the VGM affect the concentration profiles in the same way as the temperature profiles. As the pressure increases and the consumption decreases, the concentration distribution over the cross section of the reactor becomes more uniform due to stirring of the gases by recirculation, and the concentration gradients on the surface increase (Fig. 6). The latter results in an increase in the rate of deposition of the ZnSe layer.

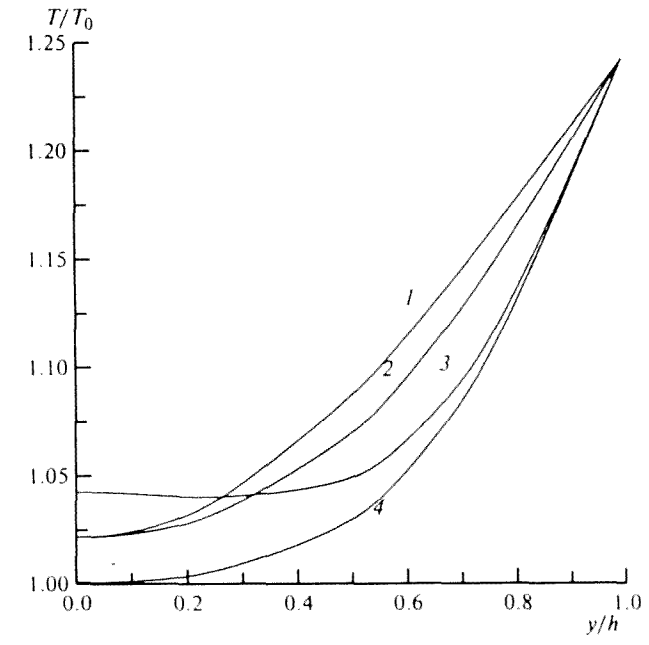

Fig. 5. Development of the temperature profile over the cross section of the reactor under various conditions of the process, P_0/kPa: 0.665 (*1*), 2.66 (*2*, *4*), 5.32 (*3*); G/m^3 h: 2.5 (*1*—*3*), 10 (*4*). T_1 = T_2 = 823 K, x = 60 cm.

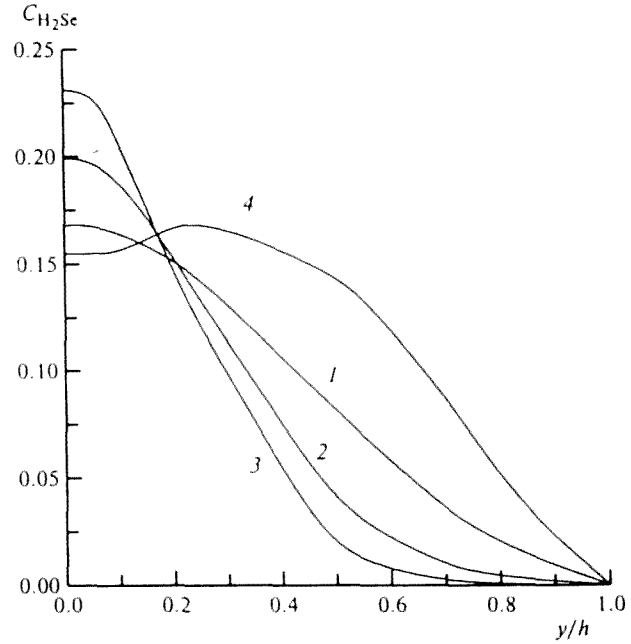

Fig. 6. Development of the profile of the concentration of H_2Se over the cross section of the reactor under various conditions of the process, P_0/kPa: 2.66 (*1*—*3*), 5.32 (*4*); G/m^3 h: 2.5 (*1*, *4*), 5 (*2*), 10 (*3*). T_1 = T_2 = 823 K, x = 60 cm.

2. Distribution of the rate of ZnS deposition under various conditions of the process and at various parameters of the reactor

The distribution of the rate of deposition of zinc selenide along the reactor depends on the same factors as the concentration, temperature, and flow rate fields considered above. The main factors are the pressure in the reactor, the chemical composition, consumption and the temperature of the VGM, the temperature of the deposition surface, and design and geometric dimensions of the reactor. The effect of these factors is complex. The extent of the effect of each of them depends on the combination of all others. For example, one cannot determine without considering this dependence, whether an increase in the consumption of the VGM results in an increase or decrease in the deposition rate and how substantial the effect of this factor is.

The growth rate was determined by the formula

$$V = \frac{6 \cdot 10^5 M_{ZnSe}}{\rho_{ZnSe} M_2} j_2,$$

where $j_2 = \rho D_2 \partial C_2/\partial y$ is the flow of the mass of H_2Se (on going from dimensions of cm s^{-1} to μm min^{-1} we introduce the factor of $6 \cdot 10^5$) and C_2 is the mass concentration of H_2Se.

The deposition rate distribution along the reactor has a maximum,[12] which shifts toward the inlet of the VGM as its consumption increases and the pressure decreases (Fig. 7). In the absence of free convection in the diffusion regime and at a constant mass concentration of the limiting component, the deposition rate is independent of the total pressure, while it increases as the pressure increases in the intermediate and kinetic regimes.[17]

In the considered case at thermodynamic equilibrium on the deposition surface and at a stoichiometric ratio of hydrogen selenide and zinc, the deposition rate is limited by the transfer of hydrogen selenide in the gas phase. A decrease in the deposition rate as the pressure in the reactor increased was experimentally observed;[4] it is likely that in these experiments the mass concentration of the limiting component changed on going from one pressure to another. In fact, the concentration of hydrogen selenide was measured[4] and was maintained constant in units of mol L^{-1}.

When the pressure increases, the number of hydrogen selenide and zinc molecules per unit gas volume remains unchanged, but the molar and mass fractions of these components decrease due to the dilution with the carrier-gas. This explains the experimentally observed[4] decrease in the deposition rate as the pressure in the reactor increases. Varying the temperatures of the deposition surface between 1023 and 1073 K exerts no noticeable effect on the growth of the layer. The same can be said about the effect of the temperature of the zinc vapor between 723 and 823 K.

Hydrogen selenide was conveyed to the reactor at room temperature and heated before injection by passing it through channels in the heated components of the reactor. Depending on the structure of the conveying channels, the temperature of H_2Se ranged within wide limits, which strongly affected the deposition rate distribution. Increasing the temperature of H_2Se at the inlet of the reactor from 823 to 373 K (Fig. 7, *c*) substantially increases the deposition rate at 2.66 kPa, while this increase is considerably weaker at 1.33 kPa. This dependence on the pressure in the reactor exerts a weak effect on the deposition rate over the whole range of the considered temperatures of H_2Se, while at 2.66 kPa its effect is substantial, and a decrease in the temperature of H_2Se favors its intensification.

Increasing the consumption of H_2Se and Zn at a constant consumption of Ar, *i.e.*, increasing the concentration of the reagents from 0 to 0.1 molar fractions,

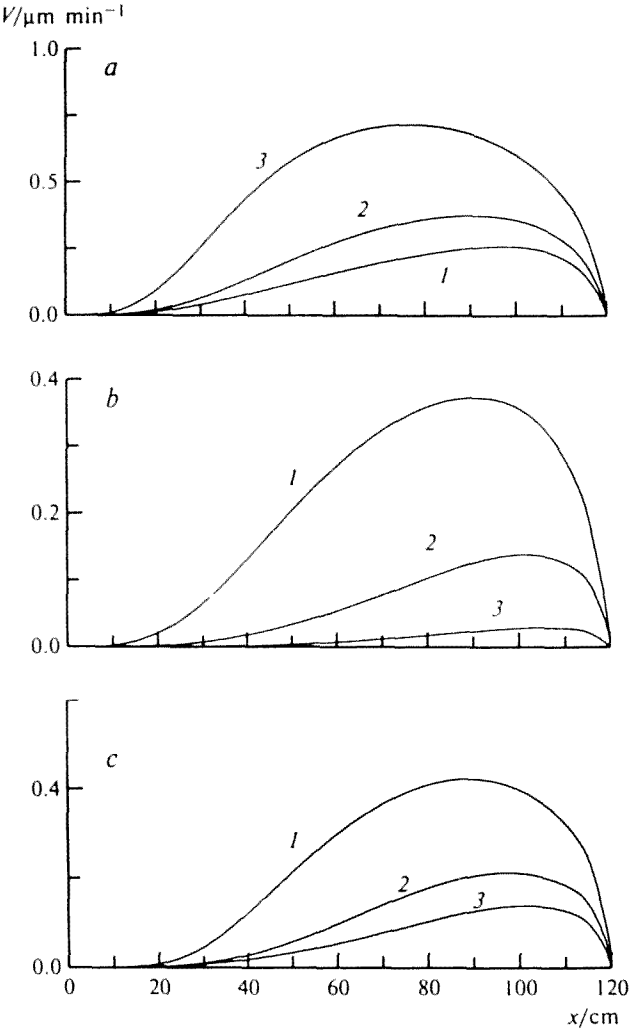

Fig. 7. Distribution of the rate of deposition of the ZnSe layer along the reactor under various conditions of the process: (*a*) at pressure, P_0/kPa: 0.665 (*1*), 2.66 (*2*), 5.32 (*3*) ($T_1 = T_2 =$ 823 K, $G = 2.5$ m^3 h); (*b*) at consumption of the VGM, G/m^3 h: 2.5 (*1*), 5 (*2*), 10 (*3*) ($T_1 = T_2 = 823$ K, $P_0 = 2.66$ kPa); (*c*) at temperature of H_2Se at the inlet, T_2/K: 373 (*1*), 573 (*2*), 823 K (*3*) ($T_1 = 823$ K, $P_0 =$ 2.66 kPa, $G = 5$ m^3 h).

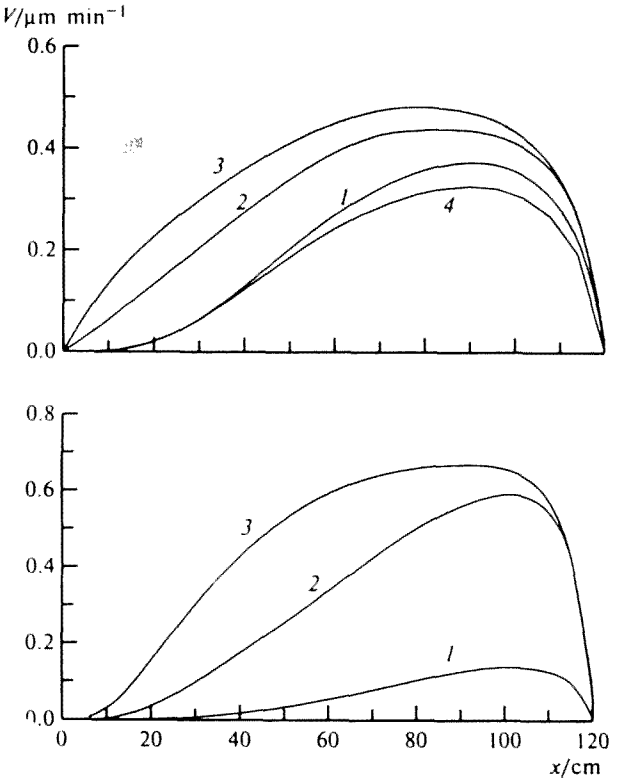

Fig. 8. Distribution of the rate of deposition of the ZnSe layer along the reactor at various parameters and geometric dimensions of the reactor ($T_1 = T_2 = 823$ K, $G = 2.5$ m^3 h, $P_0 = 2.66$ kPa): (*a*) arrangement of the peripheral port and sizes of the inlet ports: $y_{23} = 0.84$ (*1*), 0.38 (*2*), 0.2 (*3*); $y_1 = 0.06$, $y_3 - y_2 = 0.08$ (*1*—*3*); 0.015—0.02 (*4*) ($y_3 - y_2$ is the width of the peripheral port); (*b*) width of the reactor and consumption of the VGM: $h = 25$ (*1*), 12.5 cm (*2*, *3*); $G = 5$ (*1*, *2*), 2.5 m^3 h (*3*).

results in an increase in the deposition rate, but this function is not linear, because the dependence of the rate of deposition of the zinc selenide layer on the variation of the overall consumption of the VGM affects its concentration dependence.

Changes in the structural factors affect the rate of deposition to different extents. Constriction of the outlet port by 5.5 times in fact exerts no effect on the distribution of the rate of the deposition.

At the same time, a fourfold constriction of the inlet nozzles results in a decrease in the deposition rate (Fig. 8, *a*) and a decrease in the carry-over of unreacted hydrogen selenide.

Calculations were performed with $y_{23} = 0.2h$, $y_{23} = 0.34h$, and $y_{23} = 0.84h$ to estimate the effect of the arrangement of the peripheral jet. When the peripheral jet is removed from the center, the rate of deposition of the zinc selenide layer decreases along the whole channel (Fig. 8, *a*), and the carry-over of unreacted H_2Se from the reactor increases. A zone with a lower deposition rate is observed near the inlet, because the peripheral jet acts as a gas curtain impeding the movement of H_2Se to the deposition surface.

Decreasing the cross section of the reactor h from 25 to 12.5 cm substantially increases the deposition rate of zinc selenide, improves the uniformity of its distribution along the reactor (Fig. 8, *b*), and increases the degree of conversion of H_2Se. This effect increases as the consumption of argon decreases.

References

1. M. P. Braiman, E. M. Gavrishchuk, V. M. Il'in, N. M. Perepelitsa, and A. A. Pereskokov, *Vysokochistye veshchestva* [*Highly Pure Substances*], 1989, No. 1, 204 (in Russian).
2. P. L. Krupkin, E. M. Gavrishchuk, and A. Yu. Dadanov, *Vysokochistye veshchestva* [*Highly Pure Substances*], 1987, No. 6, 79 (in Russian).
3. G. G. Devyatykh, E. M. Gavrishchuk, and P. L. Krupkin, *Vysokochistye veshchestva* [*Highly Pure Substances*], 1988, No. 5, 60 (in Russian).
4. V. M. Yim and E. J. Stofko, *J. Electrochem. Soc.*, 1972, **119**, 381.
5. G. G. Devyatykh, E. M. Gavrishchuk, and A. Yu. Dadanov, *Vysokochistye veshchestva* [*Highly Pure Substances*], 1990, No. 2, 174 (in Russian).
6. P. L. Krupkin, E. M. Gavrishchuk, and A. Yu. Dadanov, *Vysokochistye veshchestva* [*Highly Pure Substances*], 1990, 112 (in Russian).
7. A. D. Gosman, W. M. Pun, A. K. Runchal, D. B. Spalding, and M. Wolfshtein, *Heat and Mass Transfer in Recirculating Flows*, Academic Press, London—New York, 1969.
8. S. Bretsznajder, *Wùasności gazów i cieczy* [*Properties of Gases and Liquids*], Naukowo-Techniczne Wydawnictwa, Warszawa (in Polish).
9. *Chemical Engineers' Handbook*, Ed. J. H. Perry, McGraw-Hill Book Company, Inc., New York, 1963.
10. R. C. Reid, T. K. Sherwood, *The Properties of Gases and Liquids*, McGraw-Hill Book Company, Inc., New York, 1958.
11. V. P. Popov and V. G. Minkina, *Teplomassoobmen-VII: Mat. VII Vsesoyuzn. konf. po teplomassoobmenu* ["*Heat and Mass Transfer-VII*," *Proc. VII All-Union Conf. on Heat and Mass Transfer*], Minsk, 1984, **8**, 122 (in Russian).
12. V. G. Minkina and V. P. Popov, *Teoreticheskie osnovy khimicheskoi tekhnologii* [*Theoretical Foundations of Chemical Technology*], 1994, **28**, 48 (in Russian).
13. M. N. Vladyko, A. A. Kolchin, and V. A. Tarchenko, *Poverkhnost'* [*Surface*], 1987, No. 9, 133 (in Russian).
14. L. M. Kulikov, *Izv. Akad. Nauk SSSR, Neorganicheskie materialy* [*Bull. Akad. Nauk USSR, Inorganic Materials*], 1982, **18**, 899 (in Russian).
15. A. Yu. Dadanov, E. M. Gavrishchuk, A. N. Kolesnikov, N. A. Sheveleva, and S. V. Yan'kov, *Vysokochistye veshchestva* [*Highly Pure Substances*], 1989, No. 6, 53 (in Russian).
16. W. M. Yim and E. J. Stofko, *J. Electrochem. Soc.*, 1972, 381.
17. V. G. Minkina and V. P. Popov, *Izv. Akad. Nauk, Neorganicheskie materialy* [*Bull. Akad. Nauk USSR, Inorganic Materials*], 1992, **28**, 5 (in Russian).
18. G. G. Devyatykh, A. Yu. Dadanov, and E. M. Gavrishchuk, *Dokl. Akad. Nauk*, 1990, **311**, 368 [*Dokl. Chem.*, 1990, **311** (Engl. Transl.)].

Received May 15, 1995;
in revised form January 10, 1996